

E. de la Luna, G. Saibene, H. Thomsen, P.J. Lomas, D.C. McDonald, T. Eich,  
M. Beurskens, A. Boboc, C. Giroud, S. Devaux, L. Garzotti, J. Lonroth,  
I. Nunes, V. Parail, R. Sartori, E.R. Solano, I. Voitsekhovitch  
and JET EFDA contributors

# Effect of ELM Mitigation on Confinement and Divertor Heat Loads on JET

“This document is intended for publication in the open literature. It is made available on the understanding that it may not be further circulated and extracts or references may not be published prior to publication of the original when applicable, or without the consent of the Publications Officer, EFDA, Culham Science Centre, Abingdon, Oxon, OX14 3DB, UK.”

“Enquiries about Copyright and reproduction should be addressed to the Publications Officer, EFDA, Culham Science Centre, Abingdon, Oxon, OX14 3DB, UK.”

The contents of this preprint and all other JET EFDA Preprints and Conference Papers are available to view online free at [www.iop.org/Jet](http://www.iop.org/Jet). This site has full search facilities and e-mail alert options. The diagrams contained within the PDFs on this site are hyperlinked from the year 1996 onwards.

# Effect of ELM Mitigation on Confinement and Divertor Heat Loads on JET

E. de la Luna<sup>1,2</sup>, G. Saibene<sup>3</sup>, H. Thomsen<sup>4</sup>, P.J. Lomas<sup>5</sup>, D.C. McDonald<sup>5</sup>, T. Eich<sup>6</sup>,  
M. Beurskens<sup>5</sup>, A. Boboc<sup>5</sup>, C. Giroud<sup>5</sup>, S. Devaux<sup>6</sup>, L. Garzotti<sup>5</sup>, J. Lonroth<sup>7</sup>,  
I. Nunes<sup>8</sup>, V. Parail<sup>5</sup>, R. Sartori<sup>3</sup>, E.R. Solano<sup>2</sup>, I. Voitsekhovitch<sup>5</sup>  
and JET EFDA contributors\*

***JET-EFDA, Culham Science Centre, OX14 3DB, Abingdon, UK***

<sup>1</sup>*EFDA-JET CSU, Culham Science Centre, OX14 3DB, Abingdon, OXON, UK*

<sup>2</sup>*Laboratorio Nacional de Fusión, Asociación EURATOM-CIEMAT, Madrid, Spain*

<sup>3</sup>*Fusion for Energy Joint Undertaking, Barcelona, Spain*

<sup>4</sup>*Max-Planck-Institut für Plasmaphysik, EURATOM-Assoziation, Greifswald, Germany*

<sup>5</sup>*EURATOM-CCFE Fusion Association, Culham Science Centre, OX14 3DB, Abingdon, OXON, UK*

<sup>6</sup>*Max-Planck-Institut für Plasmaphysik, EURATOM-Assoziation, Garching, Germany*

<sup>7</sup>*Helsinki University of Technology, Association EURATOM-TEKES, Finland*

<sup>8</sup>*Associação EURATOM/IST, Instituto de Plasmas e Fusão Nuclear, Instituto Superior Técnico,  
Av Rovisco Pais, 1049-001 Lisbon, Portugal*

*\* See annex of F. Romanelli et al, "Overview of JET Results",  
(23rd IAEA Fusion Energy Conference, Daejeon, Republic of Korea (2010)).*

Preprint of Paper to be submitted for publication in Proceedings of the  
23rd IAEA Fusion Energy Conference, Daejeon, Republic of Korea  
(10th October 2010 - 16th October 2010)



## **ABSTRACT.**

In JET several techniques have demonstrated their potential for controlling the frequency and size of type I ELMs, including static external perturbation of the edge magnetic field using the Error Field Correction Coils (EFCCs) and ELM magnetic triggering by fast vertical plasma movements ('vertical kicks'). The aim of this paper is to compare the performance of the different ELM mitigation techniques in terms of both the reduction of ELM size and the impact of each control method on plasma confinement and divertor heat loads. We find that the reduction in ELM size (up to a factor of 3), independently of the method used, is always accompanied by a reduction in pedestal pressure (mainly due to a loss in density) with only a moderate (10-15%) decrease of the stored energy. Key issues have been examined such as the behaviour of the density loss and the confinement degradation with the increase in ELM frequency, the impact of mitigation on the power required for steady state operation with regular Type I ELMs and the potential of using EFCCs for ELM mitigation in helium plasmas. The results of these experiments are discussed and their implications for ITER highlighted.

## **1. INTRODUCTION**

One of the critical issues for the plasma facing components in ITER is the high transient heat loads associated with the type I Edge Localized Modes (ELMs), which, if not addressed, can lead to rapid erosion of the divertor plates. This has stimulated worldwide research on different methods to eliminate or at least strongly reduce the ELM energy losses while maintaining adequate confinement. Taking into account that ITER will require reliable ELM control over a wide range of operating conditions, including a wide range of  $q_{95}$ , it is required to develop a suite of different techniques that could contribute to that task.

Two techniques have been successfully used at JET for ELM mitigation: static external perturbations of the edge magnetic field generated by using the Error Field Correction Coils (EFCCs) and ELM magnetic triggering by fast vertical movements of the plasma column ('vertical kicks'). It has been shown that by using plasma kicks, generated by fast radial field variations using the vertical stability control system, is possible to trigger at frequencies higher than the natural ELM frequency in Type I ELMy H-modes. The magnetic triggering requires a minimum kick size that depends on plasma parameters and is only efficient when the plasma moves towards the X-point [1]. ELM mitigation using EFCCs, has also been successfully demonstrated in JET, using both  $n = 1$  and  $n = 2$  configurations [2,3].

The aim of this paper is to compare the performance of these two ELM mitigation methods in terms of both the reduction of ELM size and their impact on plasma confinement and divertor heat loads. To that end a dedicated set of discharges was performed focused on integrating kicks and EFCCs into a similar plasma scenario. In addition, the potential of using EFCCs for ELM mitigation in helium plasmas was also explored in JET, and a comparison of those results with the effects observed in deuterium plasmas is reported here.

## 2. EXPERIMENT OVERVIEW

In this set of experiments, a standard unfuelled Type I ELMy H-mode at high triangularity ( $\delta_{ave} = 0.43$ ), with the plasma shape optimized for infrared measurements and safety factor  $q_{95} = 3.6-3.9$  (2MA/2.2-2.4T) was established for approximately 2.5 sec before applying kicks and/or EFCCs. The heating power ( $P_{NBI} = 7-12$  MW,  $P_{ICRH} = 1-2$  MW) was adjusted to produce plasmas with low ELM frequency,  $f_{ELM} \sim 7-15$  Hz, thus maximizing the increase in ELM frequency during the application of the mitigation methods. For the experiments reported here an increase in ELM frequency up to a factor of 5 with kicks (limited to  $f_{kick} = 60$  Hz due to technical reasons) and  $\sim 3.5$  with the EFCCs was obtained. In the case of the EFCCs, the increase in ELM frequency is almost independent on the coils configuration ( $n = 1, 2$ ) or the EFCC current ( $I_{EFCC} < 3$  kA) but it depends strongly on the  $q_{95}$  value [4]. We find that there is a minimum EFCC current needed for triggering the changes in ELM characteristics [3].

The plasma response to the application of both ELM control method shares common features. For both techniques the increase in  $f_{ELM}$  is associated with a decrease in the prompt energy losses caused by the ELMs and in the resulting peak divertor heat flux. The reduction in ELM size is accompanied by a reduction in edge and core density (the so-called ‘density pump-out’) which reduces the edge collisionality. In these high triangularity plasmas the pedestal density decreases from  $\sim 70\%$  to  $\sim 40-50\%$  of the Greenwald limit ( $n_{GWL}$ ) with little overall change in the shape of the density profile. In response to the density loss, the edge electron (and ion) temperature remains constant or even increases ( $\sim 15\%$ ). This in turns results in a reduction of electron edge pressure of  $\sim 15\%$ . The main difference between kicks and EFCCs resides in the toroidal rotation profile. Toroidal rotation braking (up to 50% reduction affecting the whole plasma radius) is observed when EFCCs are applied to the discharge [3]. In the case of kicks a reduction in edge rotation ( $\sim 25\%$ ) is observed associated with an increase in ELM-induced momentum losses [5].

The application of EFCCs and kicks reduces the ELM size and increases their frequency. Similar behaviour is seen by adding gas fuelling into an ELMy H-mode plasma. For mitigated ELMs we find an inverse proportionality between  $f_{ELM}$  and the fraction of the pedestal stored energy lost during an ELM ( $\Delta W_{ELM}/W_{ped}$ ) similar to what is typically obtained for spontaneous ELMs in plasmas with and without gas fuelling [6] (see figure 1). The reduction of ELM size seen during the mitigation phase is due to a decrease in the amplitude of the temperature perturbation ( $\Delta T_e/T_e$ ) varies from 40% to 10% for the set of data shown in figure 1). The relative density losses remain nearly constant (5-10% from interferometer measurements), only decreasing weakly with the ELM frequency, as normally seen in ELMy H-modes [7]. In general, no significant difference between spontaneous and mitigated ELMs has been found with respect to ELM characteristics such as the ELM-affected region (typically  $\sim 20-25\%$  of the plasma radius from ECE measurements [7]) or the filamentary structure of the power deposited in the divertor.

There is, however, a difference between mitigated and spontaneous ELMs as shown in figure 2. Since mitigated ELMs are associated with a decrease in pedestal density at constant pedestal

temperature they do not follow the trend of increasing ELM size with decreasing collisionality as observed in a wide range of ELMy H-mode discharges [7].

### 3. EFFECT OF ELM MITIGATION ON ELMS AND ENERGY AND PARTICLE CONFINEMENT

Figure 3 illustrates the impact on confinement of the different ELM mitigation schemes explored on JET for the same data set shown in figure 1. The data points shown are averaged over selected stationary time intervals. The thermal stored energy decreases by 10-15% with the application of any of the mitigation techniques, mainly due to an increase in convective losses that reduces the core density up to 30%. However, due to the positive density dependence of the energy confinement time ( $\tau_E \sim n^{0.4}$ ) predicted by the IPB98(y,2) scaling, the unfuelled H-mode plasmas in the mitigated phase exhibit good confinement ( $H_{98}=1-1.1$ ) with  $n_{e,ped}/n_{GW} = 0.4-0.5$ . Gas fuelling and pellet injection [3] have been used to restore the density loss caused by the mitigation. Applying EFCCs to the gas fuelled plasma is found to act essentially additively on the background ELM frequency. ELM pacing with kicks is technically limited to 60 Hz and this is typically smaller than the ELM frequency achieved in gas fuelled plasmas. As it can be seen in figure 3, it is possible to recover the density loss caused by the mitigation method but the edge and central temperature reduce and the global confinement decreases to those of the standard fuelled H-mode plasmas.

More insight on the mechanism responsible of the density pump-out can be gained from the analysis of the density loss as a function of the ELM frequency. The density loss ( $\Delta n_{e,mit} = n_e^{initial} - n_e^{mit}$ ) is determined from the difference between density profiles before and during the application of the kicks or EFCCs (at the end of the mitigation phase). The data is obtained from Thomson Scattering measurements just before the ELMs and averaged over 5-10 similar ELMs. As can be seen in figure 4, the relative density losses increase with the increase in ELM frequency ( $f_{ELM}^{mit}/f_{ELM}^0$ , where  $f_{ELM}^0$  and  $f_{ELM}^{mit}$  are the ELM frequencies for mitigated and spontaneous ELMs before kicks or EFCCs are applied, respectively). This observation is particularly clear for the experiments with kicks, where the ELM frequency can be externally controlled by varying  $f_{kick}$ , thereby suggesting a direct correlation between the density pump-out and the ELM particle losses. Contrary to what happens with the ELM conductive losses ( $\Delta T_{ELM} \sim 1/f_{ELM}$ ), ELM convective losses are weakly dependent on ELM frequency and therefore the ELM-induced particle outflux ( $f_{ELM} \times \Delta N_{ELM}$ ) increases with increasing  $f_{ELM}$ . This explanation can be directly applied to the kicks, which are intermittent by nature and can only affect the transport by triggering extra ELMs but not between ELMs. This is corroborated by the fact that the rate at which the stored energy recovers in between ELMs is essentially the same for spontaneous and triggered ELMs. For the EFCCs experiments described here (at fixed  $q_{95}$ ) the range of variation in  $f_{ELM}^{mit}/f_{ELM}^0$  is too small to extract any conclusion. However, similar trend of increasing density losses with increasing ELM frequency can be observed in recent EFCCs experiments at low triangularity, where  $f_{ELM}$  is varying by scanning  $q_{95}$  ( $q_{95} \sim 4.2-4.8$ ) [8]. This is again in agreement with the aforementioned argument, suggesting that both kicks

and EFCCs affect the ELMs by modifying the edge stability but not the background transport. This is further supported by the fact that no significant difference has been observed in the recovery rate of the pressure profile as the pedestal builds up between ELMs with and without EFCCs [9].

Finally, the impact of ELM mitigation on the H-mode confinement with respect to its potential extension towards higher ratios  $f_{\text{ELM}}^{\text{mit}}/f_{\text{ELM}}^0$  has been investigated. EFCCs are excluded from this analysis due to the limited range of ELM frequency achieved in the experiments reported here. Figure 5 shows that the increase in ELM frequency invariably leads to some confinement deterioration. One can see that most of the reduction in the stored energy is obtained at  $f_{\text{ELM}}^{\text{mit}}/f_{\text{ELM}}^0 \sim 3$  and it tends to saturate at higher values of  $f_{\text{ELM}}^{\text{mit}}/f_{\text{ELM}}^0$ . At a given increase in ELM frequency the loss in confinement is larger for gas fuelled plasmas. In contrast to the ELM pacing methods, such as kicks or pellets, a further increase in  $f_{\text{ELM}}$  by means of gas fuelling can only be obtained at a price of a strong confinement degradation which eventually causes a back transition from H- to L-mode.

#### 4. ELM MITIGATION AND DIVERTOR HEAT LOADS

A key ingredient in the ELM mitigation experiments in JET is the possibility of diagnosing the ELM-resolved heat load profiles on the outer divertor target by a fast high resolution infrared camera [10]. Figure 6 shows the heat flux (normalized to the average value obtained for the larger ELMs) and the effective width of the heat flux profile (wetted area) at ELM peak and inter-ELM times for three pulses where EFCCs were applied. In these experiments, spontaneous and mitigated ELMs are obtained in the same pulse at constant power. It was found that the wetted area increases with relative ELM size [11,12], in agreement with results obtained for spontaneous ELMs (fuelled and unfuelled plasmas) [10,13]. A similar behaviour is also found for the small ELMs obtained with the enhanced toroidal ripple [14] in JET and with the edge Resonant Magnetic Perturbations (RMP) in DIID-D [15]. In spite of this variation in the wetted area, a reduction in the ELM peak heat flux as the ELM size decreases is still observed. These results also show that the wetted area for mitigated ELMs is typically 1.5-3 times larger than the inter-ELM values and this broadening increases as the ELM size increases[10].

#### 5. EFFECT OF ELM MITIGATION ON STEADY STATE OPERATION IN TYPE I ELMY H-MODES

So far, the highest level of confinement for H-mode operation in present tokamaks is obtained in the presence of regular type I ELMs. In the case of JET, heating powers ( $P_{\text{IN}}$ ) well above the L-H transition power threshold ( $P_{\text{LH}}$ ) are necessary to maintain stationary Type I ELMy H-modes. Typically this factor for JET is  $P_{\text{IN}}/P_{\text{LH}} > 1.4$  at high triangularity and may be higher at lower triangularity [16]. In ITER the power available for access to H-mode is limited. In many scenarios the RMP coils will be used soon after the L-H transition in order to secure an efficient ELM control, therefore it is important to determine whether the power required to reach good confinement is influenced by the ELM mitigation techniques. This has been studied in JET by applying EFCCs



( $n = 1,2$ ) and kicks in discharges with heating power marginally above the power required to obtain Type I ELMy H-mode.

In the case of the EFCCs, the character of the ELMs can change dramatically with only a small change in the power margin above PLH, as can be seen in figure 7. In the two pulses shown in the figure, the power is sufficient to maintain the stationary Type I ELM regime before the EFCCs are turned on. At the highest heating power, with  $P_{\text{loss}}/P_{\text{LH}} \sim 1.6$  ( $P_{\text{loss}} = P_{\text{abs}} - \partial W/\partial t$ ) using the Martin08 scaling [17], the application of the EFCCs is soon followed by the characteristic mitigation signatures, typically an increase in ELM frequency and a reduction in density that reaches a new stationary value (see figure 7c). However, a small reduction in heating power (from 11.3 to 10.2MW) causes the ELM behaviour to change significantly during the phase when the coils are on (see figure 7b). The average period between the ELMs increases and the ELMs become more compound, with large ELMs followed by a short period of more frequent ELMs with lower amplitude. These large ELMs are associated with rapid drops of both the density and the stored energy (not shown) and the confinement continuously degrades during the EFCC phase. As it can be seen in the figure, the ELM frequency is recovered when the EFCC current is turned off. Similar behaviour can also be observed by increasing the magnetic field at constant input power during the application of EFCCs, thus decreasing the power margin above threshold. The sequence of H-mode phases described above, from regular type I ELMs, to compound ELMs, to ELM free phases, is normally associated with a reduction in the loss power or an increase in PLH. No clear changes in the plasma profiles prior the change in the ELM behaviour are detected, within the resolution of the instruments, except in the rotation profile that decreases as soon as the coils are turned on. It follows from these results that more power is necessary to maintain type I ELMs when EFCC are applied. Similar results have been obtained in MAST [18]. Given the different characteristics of the coils in MAST (internal with  $n = 3$ ) and JET (external with  $n = 1,2$ ), it is suggested that these effects must be related to a common mechanism and not to a specific feature of the perturbation spectrum, such as the reduction in edge toroidal rotation observed in both devices through its impact on the edge radial electric field. Unfortunately this issue has not been yet resolved due to limitations on experimental time and will be addressed in future campaigns.

In contrast, there is experimental evidence that the power required to maintain in steady state an ELMy H-mode with type I ELMs can be reduced by using vertical kicks. An example is shown in figure 7. This is a low triangularity pulse at low input power ( $P_{\text{NBI}} = 6.3\text{MW}$ ), where kicks are applied during the second half of the heating phase. In this case the input power is not enough to attain steady state conditions and spontaneous H-L transitions appear at the beginning of the discharge. During the ELM-free period the core (and edge) density rises in an uncontrollable way whereas the stored energy saturates. One can see that, even in these conditions, kicks ( $f_{\text{kick}} = 10\text{Hz}$ ) are efficient in triggering ELMs. The increase in the number of ELMs makes particle density control possible, ultimately leading to a stationary behaviour and good confinement ( $H_{98y} = 1.1$ ) with  $P_{\text{loss}}/P_{\text{LH}} \sim 1.2$ . Both, the  $T_e$  and  $n_e$  at the top of the pedestal just before the ELM crash, and therefore the maximum

edge pressure gradient (assuming constant pedestal width [19]), are very similar for the naturally occurring big ELMs in the first phase of the discharge and the small triggered ELM. This implies that the maximum achievable pressure gradient might be set by the peeling-ballooning stability limit but the ELM trigger mechanism for these two types of ELMs is different. However, the question of why the abrupt transition to L-mode is seen after the spontaneous ELMs still remains. As triggered ELMs produce smaller energy losses, they are less likely to reach a pedestal temperature after the ELM crash near to the critical temperature for H→L transition, which has been often suggested as a possible candidate to explain such kind of transition.

## 6. ELM MITIGATION IN <sup>4</sup>HE PLASMAS

Operation with helium plasmas is the main candidate for H-mode related studies during a low activation phase of ITER operation. During 2009, a short and very focused helium campaign was carried out in JET to address specific issues of H-mode physics (see also [20]). Amongst others, a series of dedicated experiments aimed at comparing the effect of the EFCCs on the ELMs in matched deuterium (D) and helium (<sup>4</sup>He) plasmas were performed to document whether the results obtained in <sup>4</sup>He in ITER could then be extrapolated to D-T plasmas. For these experiments both JET beam boxes were converted to pure helium injection. D and <sup>4</sup>He H-mode discharges were obtained with the same shape ( $\delta = 0.4$ ) that those described in the previous sections but with a slightly lower magnetic field ( $B = 2\text{T}$ ,  $1.8\text{MA}$   $q_{95} = 3.6$ ). The He purity in these experiments was 85-93%. The main observations in these experiments are summarized in figure 8, where two similar He pulses ( $q_{95} \sim 3.4-3.6$ ) with and without EFCCs ( $n = 2$ ,  $I_{\text{EFCC}} = 3\text{kA}$ , maximum EFCC current) applied are compared. In the case of <sup>4</sup>He, the plasma does not reach stationary conditions and the ELM frequency continuously increases throughout the pulse. This is a typical feature in these JET experiments caused by the low active He pumping, irrespective of the use of the EFCCs. As it can be seen in figure 9, a very similar increase in ELM frequency is observed with and without EFCCs in the case of the <sup>4</sup>He plasmas. For comparison, the matched D pulse, with similar  $n_{e,\text{ped}} \sim 4.5-5 \cdot 10^{19} \text{ m}^{-3}$  but higher  $T_{e,\text{ped}}$  than the <sup>4</sup>He pulse (1keV for D and 0.5keV for He) is shown in figure 9 together with an additional D pulse with strong external gas fuelling.

So far there is no explanation for the different plasma behaviour when the EFCCs are applied between the D and <sup>4</sup>He plasmas. However, it should be noted that the effectiveness of the EFCCs for ELM mitigation in D plasmas decreases significantly (or even disappears) as the edge recycling increases, either by gas puffing or in plasmas with smaller pumping or reduced distance to the wall. The difference between strongly fuelled and unfuelled D plasmas can be seen in figure 10. In both the D fuelled discharge and <sup>4</sup>He H-modes the braking of the rotation is still seen but all the other features characteristic of ELM mitigation (increase in ELM frequency and density pump-out) are absent. From this data we conclude that the lack of ELM mitigation observed in <sup>4</sup>He plasmas may not be specific to <sup>4</sup>He but related to the higher recycling fluxes (by gas fuelling or wall recycling) obtained in the <sup>4</sup>He pulses compared to that obtained in the unfuelled D reference pulses.

## 7. DISCUSSION AND CONCLUSIONS

This paper reports on the use of EFCCs and ‘vertical kicks’ to investigate the impact of ELM mitigation on plasma confinement and power divertor loads. For kicks and EFCCs the reduction in ELM losses is accompanied by edge and core density loss, resulting in a pedestal at low collisionality, which demonstrates that the trend of increasing ELM size with decreasing collisionality, which is quite robust in standard H-mode operation, can be broken. There is experimental evidence that both kicks and EFCCs modify the edge stability but not the background transport and therefore ELM-induced particle losses play the dominant role in the enhanced particle transport observed in these experiments. The precise mechanism through which kicks (via changes in edge current and/or plasma shape) and EFCCs affect the edge stability is still unknown. Analyse of the edge stability including 3D effects self-consistently are needed for a more quantitative understanding of these observations. It is worth mentioning that in JET no reduction in the density is observed when EFCCs are applied in L-mode plasmas and strike point splitting (measured from the outer divertor heat flux profiles) is only observed in L-mode plasmas but not in H-mode in spite of being predicted by vacuum field modelling [21]. All these findings are consistent with modelling results indicating that the applied magnetic perturbation can be screened by the plasma rotation [21] so that the width of the stochastic magnetic layer at the edge is smaller than that expected from vacuum calculations. For coming experiments in JET it is planned to increase the maximum current in the EFCCs up to 6 kA thereby increasing the size of the edge perturbation. It should be noted that the comparison between JET and DIII-D results, where ELM suppression has been observed [22], is not straightforward. The level of edge ergodization as well as the perturbation spectrum is very different in JET and DIII-D and therefore a different mechanism could be responsible of the density pump-out observed in DIII-D [22] during the mitigation phase (when  $q_{95}$  is outside the resonance window for ELM suppression). In any case, the question of how to maintain the density in steady state during the ELM suppression phase in DIII-D still remains. JET results show that, regardless the method employed, a decrease in ELM size by increasing  $f_{ELM}$  invariably leads to a confinement deterioration that tends to saturate when the ELM frequency increases by more than a factor of 3. Further experiments are planned to extend the experimental database to larger increases in ELM frequency. Although the impact on the global confinement of the mitigation methods in ITER remains to be estimated, the confirmation of this trend would have positive implications for ITER, where an increase in ELM frequency  $\sim 20-30$  is foreseen. With regard to the heat divertor loads, we have found that the ELM heat flux profile is always broader than the the inter ELM profile and its effective width scales with ELM size independent of the method used to reduce the ELM size (gas, ripple or ELM mitigation). Interestingly, for ripple ( $\sim 1\%$ ) and EFCCs the small ELMs are obtained at low pedestal collisionality, whereas in the case of gas fuelled plasmas, the reduction in ELM losses is accompanied by an increase in collisionality. Therefore, it is concluded that the change in the wetted area with ELM size is independent on the pedestal collisionality. A more detailed discussion of how these new experimental findings affect the ELM control requirements for ITER

can be found in [23]. It was found that both kicks and EFCCs can influence the power requirements to maintain steady-state type I ELMs. Kicks have shown to be capable of triggering ELMs during otherwise ELM-free periods of the discharge achieving stationary conditions at much lower input power above PLH compared to standard H-mode discharges. This effect is not observed with EFCCs, moreover the minimum Ploss/PLH value for access to the regular type I ELMy H-mode regime increases. This is an important issue for ITER and will be addressed in future campaigns. Finally, experiments carried out in  $^4\text{He}$  plasmas showed that, in contrast to what it is observed in D unfuelled plasmas, the ELM behaviour and the plasma density are unaffected by the EFCCs coils (up to the maximum explored value of  $I_{\text{EFCC}} = 3\text{kA}$ ). Similar results were obtained in D plasmas with high recycling (lower edge temperature or higher collisionality), obtained either by adding gas fuelling or increasing the wall recycling, and therefore are not specific of  $^4\text{He}$  plasmas. Further experiments are required to develop a detailed understanding of these observations.

### ACKNOWLEDGMENTS.

This work was supported by EURATOM and carried out within the framework of the European Fusion Development Agreement. The views and opinions expressed herein do not necessarily reflect those of the European Commission

### REFERENCES

- [1]. E.de la Luna et al., 36th EPS Conf. on Plasma Physics 2008 (Sofia, Bulgaria)
- [2]. Y. Liang et al., Physical Review Letters **98** (2007) 265004
- [3]. Y. Liang et al., Nuclear Fusion **50** (2010) 025013
- [4]. Y. Liang et al., Physical Review Letters **105** (2010) 065001
- [5]. T. Versloot et al., Plasma Physics and Controlled Fusion **52** (2010) 45014
- [6]. A. Herrmann et al., Plasma Physics and Controlled Fusion **44** (2002) 883
- [7]. A. Loarte et al., Plasma Physics and Controlled Fusion **44** (2002) 1815
- [8]. Y. Liang et al., This conference (IAEA EXS/P3-04)
- [9]. Y. Liang et al., Proc. 19th ITC Conference (2010) (submitted to Plasma and Fusion Research)
- [10]. T. Eich et al., 19th PSI conference (San Diego, USA) 2010
- [11]. E. de la Luna et al., 51th APS (Atlanta, USA) 2009
- [12]. S. Jachmich et al., 19th PSI conference (San Diego, USA) 2010
- [13]. H. Thomsen et al., This conference (IAEA EXD/6-6Rb)
- [14]. H. Thomsen et al., 36th EPS (Sofia Bulgaria) 2009
- [15]. M.W. Jakubowski et al., Nuclear Fusion **49** (2009) 095013
- [16]. R. Sartori et al., Plasma Physics and Controlled Fusion **46** (2004) 723
- [17]. Y. Martin et al., J. Phys. Conf. Ser. **123** (2008) 012033
- [18]. A. Kirk et al., Nuclear Fusion **50** (2010) 034008
- [19]. M. Beurskens et al., Plasma Physics and Controlled Fusion **51** (2009) 124051

- [20]. D. McDonald, This conference (IAEA 2010 EXC/2-4Rb)  
 [21]. E. Nardon et al., 19th Plasma Surface Interaction Conference (San Diego, USA) 2010  
 [22]. T.E. Evans et al., Nature Physics **2**, (2006) 419  
 [23]. A. Loarte et al., This conference

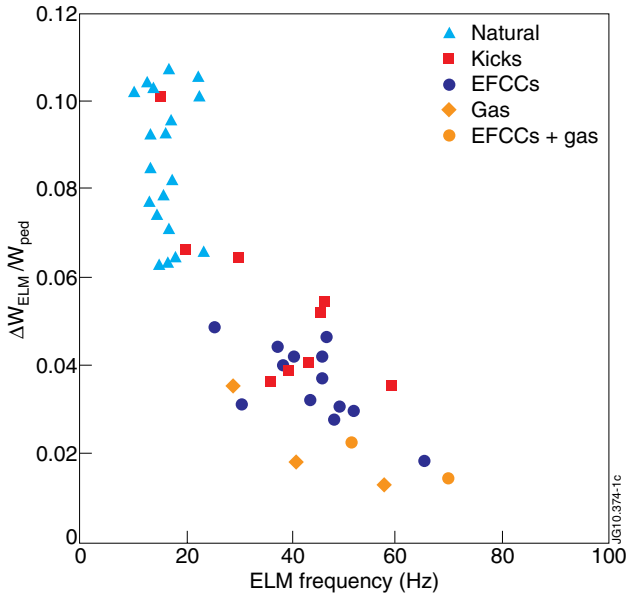


Figure 1: Normalized ELM energy loss (to the pedestal stored energy) versus ELM frequency for different ELM mitigation methods (high  $\delta$ ,  $q_{95} = 3.6-3.9$ ).

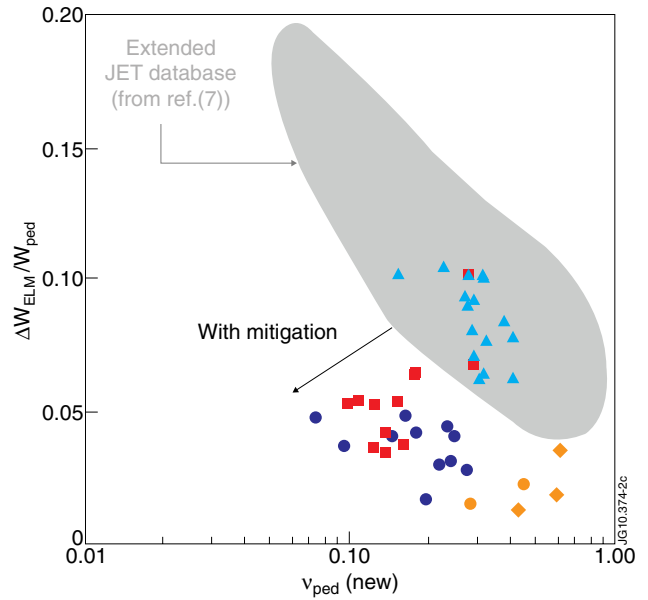


Figure 2: Normalized ELM energy loss versus pedestal collisionality for the same data set shown in figure 1.

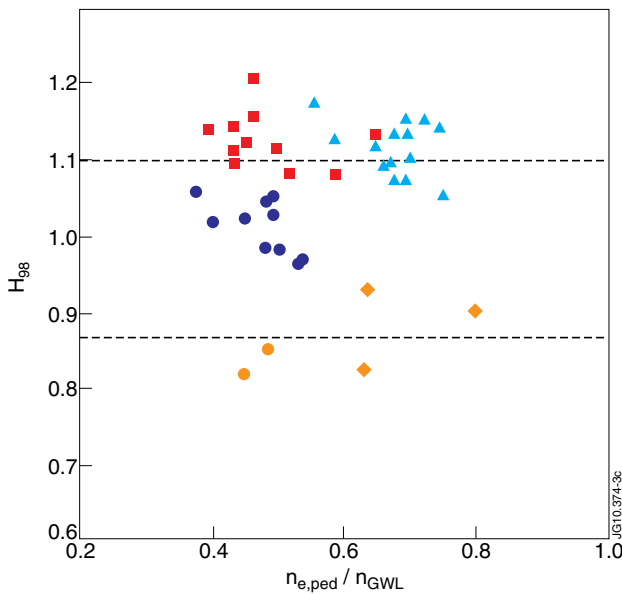


Figure 3: Energy confinement enhancement factor  $H_{98}$  versus pedestal density normalized to Greenwald density for the dataset shown in figure 1. Same colour code as figure 1.

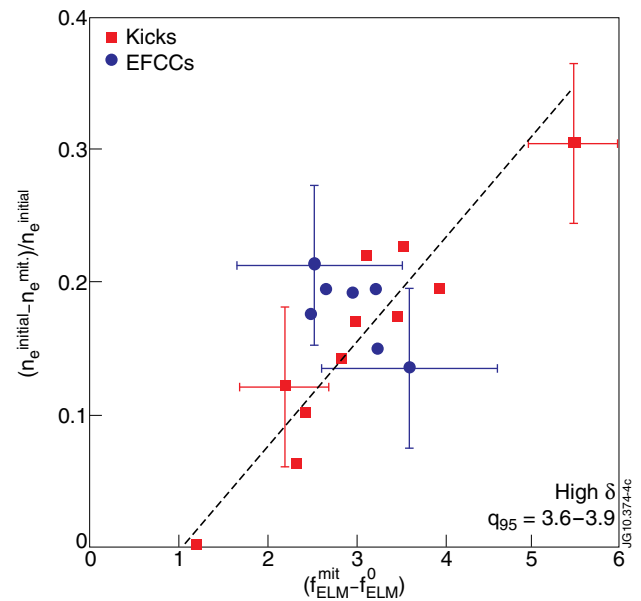


Figure 4: Density loss in the core region ( $r/a \sim 0.3$ ) normalized to the core density before kicks or EFCCs are applied versus increase in  $f_{ELM}$  (unfuelled plasmas).

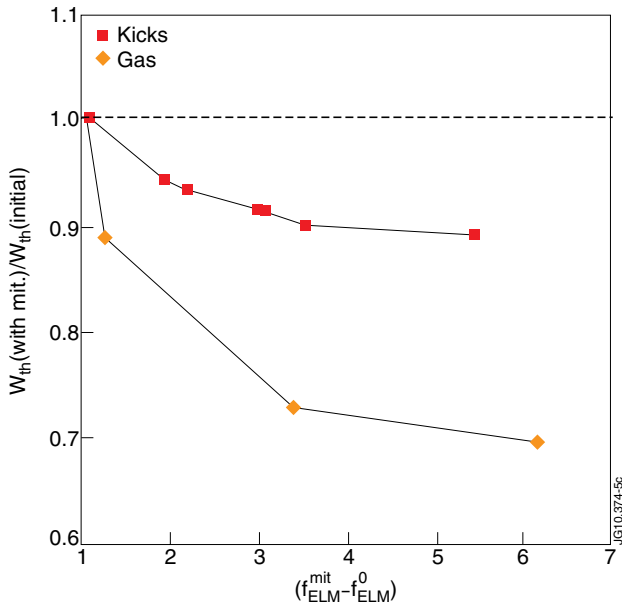


Figure 5: Ratio between the thermal stored energy during and before the application of gas and kicks versus increase in  $f_{ELM}$  for a subset of the data shown in figure 1.

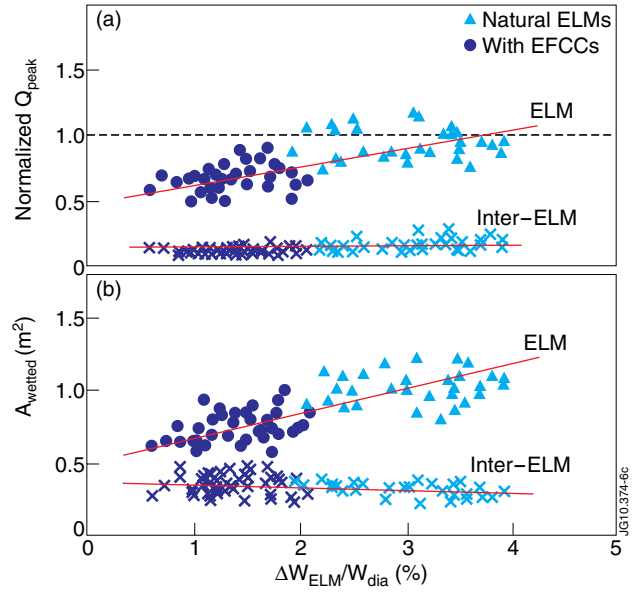


Figure 6: a) Normalized peak heat fluxes and b) wetted areas from IR outer divertor data versus relative ELM losses (normalized to  $W_{dia}$ ) for natural and mitigated (EFCCs) ELMs (unfuelled, high  $\delta$  plasmas).

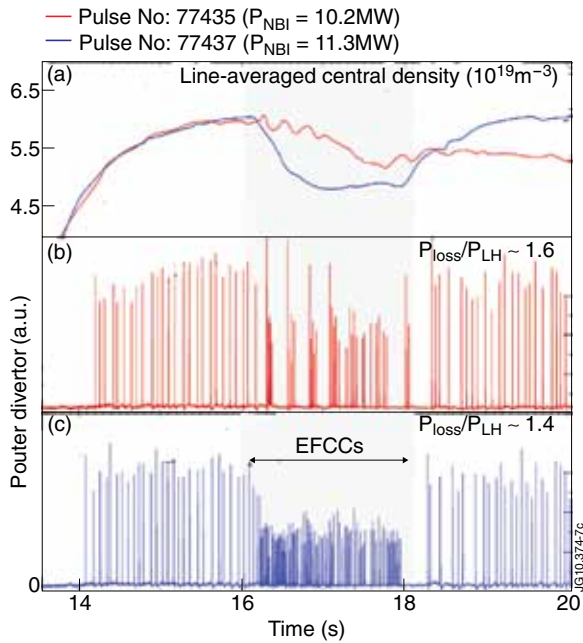


Figure 7: Effect of EFCCs on plasmas with heating power marginal above  $P_{LH}$  (high  $\delta$ , 2.2T/2MA)

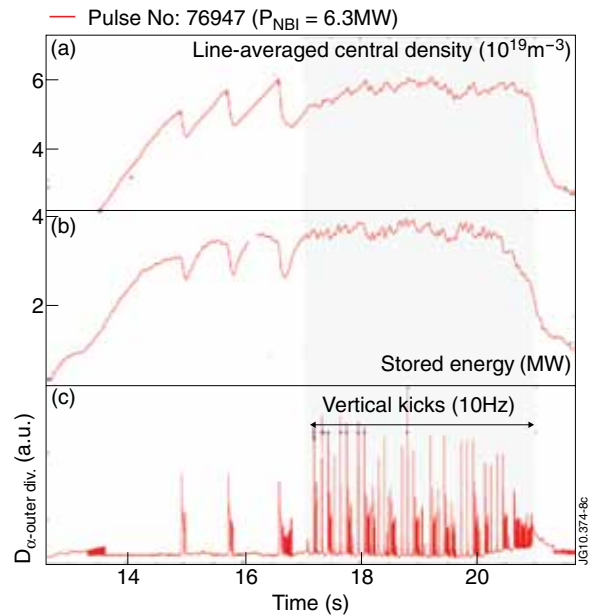


Figure 8: Effect of kicks on a plasma with heating power marginal above  $P_{LH}$  (low  $\delta$ , 2.2T/2MA)

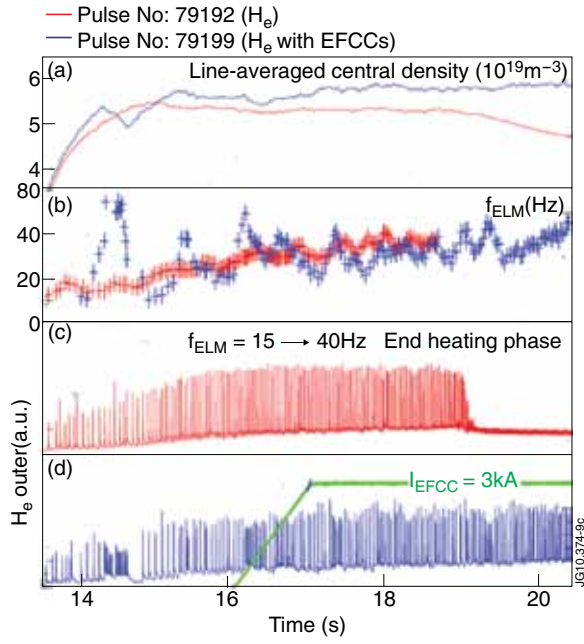


Figure 9: Time traces a) line averaged electron density, b)  $f_{\text{ELM}}$  and c,d) divertor  $\text{H}_e$  line emission for two  $^4\text{He}$  Pulse No's: 79192 (red) without EFCCs and 71999 (blue) with EFCC. ( $P_{\text{NBI}} = 12.3 \text{MW}$ , high  $\delta$ ,  $1.8 \text{T}/1.7 \text{MA}$  (c) and  $2 \text{T}/1.8 \text{MA}$  (d)).

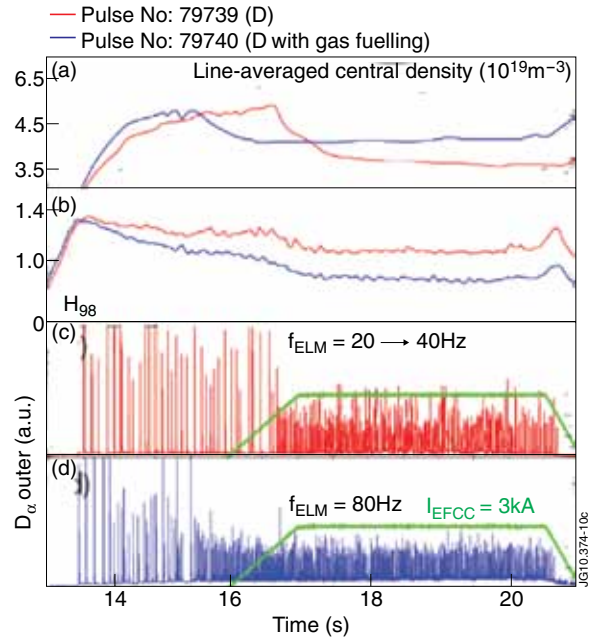


Figure 10: Time traces a) line averaged electron density, b)  $\text{H}_{98}$  factor and c,d) divertor  $\text{D}_\alpha$  line emission for two D Pulse No's: 79739 (red) unfuelled and 79740 (blue) with gas fuelling (matched parameters to  $^4\text{He}$  Pulse No: 71999).